



# Asteroseismology of Red Clump Stars as a Probe of the Dark Matter Content of the Galaxy Central Region

José Lopes<sup>1</sup> , Ilídio Lopes<sup>1</sup> , and Joseph Silk<sup>2,3,4</sup> <sup>1</sup> Centro de Astrofísica e Gravitação—CENTRA, Departamento de Física, Instituto Superior Técnico—IST, Universidade de Lisboa—UL, Av. Rovisco Pais 1, 1049-001 Lisboa, Portugal<sup>2</sup> Institut d’Astrophysique de Paris, UMR 7095 CNRS, Université Pierre et Marie Curie, 98 bis Boulevard Arago, Paris F-75014, France<sup>3</sup> Beecroft Institute of Particle Astrophysics and Cosmology, 1 Keble Road, University of Oxford, Oxford OX1 3RH, UK<sup>4</sup> Department of Physics and Astronomy, 3701 San Martin Drive, The Johns Hopkins University, Baltimore, MD 21218, USA

Received 2019 June 4; revised 2019 June 29; accepted 2019 July 8; published 2019 July 30

## Abstract

The study of dark matter (DM) captured inside stars has proved to be a viable indirect search strategy complementary to other direct searches. However, in this context, only a fraction of the rich diversity of physics found in different types of stars has been explored, with most studies addressing main-sequence stars and, particularly, the Sun. In this work we focus instead on red clump stars, i.e., core helium-burning stars located in the red end of the horizontal branch. These stars, in some cases with  $L \simeq 10^2 L_\odot$ , can be observed throughout the galaxy and thus can give us insight into the DM conditions found in situ. We consider thermally produced DM particles in the mass range 4–10 GeV with spin-independent annihilation and scattering cross-sections that are close to the observational upper limits from direct detection experiments. Our results show that the evacuation of energy via DM interactions with baryons can cease convection in the central region of the star, which will have a measurable impact on the asteroseismology of the star. This result is particularly interesting for densities that are appropriate for stars within the central few parsecs of the Milky Way. We also explore the prospect of using these effects to study the content of DM in the Milky Way core.

*Key words:* asteroseismology – dark matter – stars: horizontal-branch

## 1. Introduction

While the study of the impact of dark matter (DM) in stars has proven to be particularly fruitful for the case of the Sun (e.g., Lopes et al. 2002; Frandsen & Sarkar 2010; Taoso et al. 2010; Catena 2015; Vincent et al. 2015; Lopes & Lopes 2016), studies have mostly focused on main-sequence solar-like stars (Salati & Silk 1989; Fairbairn et al. 2008; Scott et al. 2009; Casanellas & Lopes 2013), compact stars (Isern et al. 2008; Kouvaris 2008; de Lavallaz & Fairbairn 2010), and brown dwarfs (Zentner & Hearin 2011). In this work, we are interested on the impact of DM on low-mass stars sitting in the red extremity of the horizontal branch (HB), a zone usually referred to as the red clump (RC) region in the Hertzsprung–Russell diagram, characterized by a convective helium-burning core that provides a stable source of energy (for a detailed review on RC stars, see Girardi 2016). We consider the general class of weakly interacting massive particles (WIMPs), thermally produced during the early universe with a thermally averaged annihilation cross-section  $\langle\sigma v\rangle$  defined by the relic abundance (e.g., Jungman et al. 1996, and references therein). As is the case in most experimental searches, we assume DM–baryon interactions through an effective constant cross section  $\sigma_{\text{SD/SI}}$ , which can have both spin-dependent (SD) and spin-independent (SI) components.

Experimentally, searches for WIMP interactions have been either fruitless or mutually incompatible (see Roszkowski et al. 2018, and references therein). While liquid xenon detectors have placed strong limits on SI interactions for masses around the electroweak symmetry-breaking scale ( $\sigma_{\text{SI}} < 10^{-46} \text{ cm}^2$  for  $m_\chi \sim 100 \text{ GeV}$ , where  $m_\chi$  is the DM particle mass), in the low-mass region ( $m_\chi < 10 \text{ GeV}$ ) constraints are typically weaker due to the lack of coherence effects in interactions. Luckily, this is also the parameter region for which a DM signature in an

RC star should be maximal due to its helium content ( $m_\chi \simeq m_{\text{He}}$ ). In this region, the CDMSlite germanium detectors place an upper limit of  $\sigma_{\text{SI}} < 10^{-41} \text{ cm}^2$  for  $4 \text{ GeV} < m_\chi < 10 \text{ GeV}$ . These results, however, are subject to background contamination issues or uncertainties in the high-velocity tail of the DM galactic velocity distribution.

Early works by Dearborn et al. (1990) and Renzini (1987) explored the effects of WIMPs in HB stars; however, the potential of actually using RC stars as an experimental tool to probe DM has remained unexplored. One of the reasons why these stars are such unique laboratories to probe DM interactions is that their core is mainly composed of helium, and thus the effect of interactions with helium and heavier elements is larger than stars in the main sequence, which have hydrogen-rich cores. From an observational point of view, RC stars are also very relevant. Not only are they observable throughout the Milky Way due to their brightness ( $L \sim 10^2 L_\odot$ ), they are also expected to constitute approximately 30% of the nearby population of observed red giants (Girardi 2016). Also, because they clump in a well-defined region of the color–magnitude diagram, RC stars are frequently used as accurate distance indicators to the galactic center (Paczynski & Stanek 1998), which is the region where a possible signature should be amplified due to the expected large concentration of DM. In fact, recent estimations of the DM density profile favor a DM density of  $\rho_{\text{DM}} \simeq 10^3\text{--}10^6 \text{ GeV cm}^{-3}$  within the inner parsec of the Milky Way, which is orders of magnitude above the DM density in the solar neighborhood,  $\rho_{\text{DM},\odot} = 0.4 \text{ GeV cm}^{-3}$  (Hooper 2017). Recent asteroseismic surveys have also allowed a more in-depth analysis of the interiors of RC stars. Data from missions such as *Kepler* (Mosser et al. 2014) and *CoRoT* (Hekker et al. 2009) have allowed the detection and

identification of mixed-oscillation modes on thousands of RC stars throughout the Milky Way, enabling a precise estimation of asteroseismic parameters that are sensitive to the stellar internal structure.

## 2. DM in Red Clump Stars

Particles from the DM halo can be gravitationally trapped inside stars due to energy lost in the scattering process with baryons in the stellar plasma. In the case of DM with non-negligible annihilation cross sections, the capture process will eventually be balanced by annihilation, and the number of DM particles will reach an equilibrium defined by

$$\frac{dN_\chi}{dt} = C_\odot - A_\odot N_\chi^2, \quad (1)$$

where  $C_\odot$  is the capture rate, and  $A_\odot$  is the annihilation cross section times the relative DM velocity per unit volume. In fact, evaporation, the inverse process of capture, should also be accounted in Equation (1). There has been a long discussion about the conditions for which evaporation is negligible in HB stars (Spergel & Faulkner 1988; Gould 1990). In particular, Gould (1990) has shown that, for a typical HB star with mass  $0.8 M_\odot$ , the evaporation mass, i.e., the DM mass below which evaporation is non-negligible, varies between  $m_\chi \simeq 4$  GeV and just below  $m_\chi = 10$  GeV. For this reason, we decided to cover an array of DM masses ranging from cases where, according to (Gould 1990), evaporation can be non-negligible ( $m_\chi = 4$  GeV) to cases where it is completely negligible ( $m_\chi = 10$  GeV).

Once trapped inside the star, DM particles will help the transport of energy away from hotter regions by scattering with the baryonic nuclei (Steigman et al. 1978; Spergel & Press 1985). If energy transport by DM is efficient, transport by convection in core helium-burning stars can be suppressed. Moreover, because convection is also the mechanism responsible for replenishing the burning region with helium from the inert outer central layers, the abrupt ceasing of convection can lead to an early end of the core-helium burning phase (Dearborn et al. 1990).

To model the effects of DM in stars, we have developed an extension to the widely used MESA stellar evolution code (Paxton et al. 2011, 2013, 2015, 2018), which computes the DM phenomenology, including capture, annihilation, and energy transport at each step of the evolution of the star. In our implementation, the energy transport by DM is treated as an extra energy term, as described in Scott et al. (2009). The extra energy term from DM interactions is computed and added explicitly in the MESA differential equation solver at each age step of the model. It is important to note that despite being treated as a source term, there is no outflow of energy due to transport by DM (in the approximation where evaporation is negligible). This transport effect should not be confused with energy production in DM annihilations (e.g., Casanellas & Lopes 2011), which is not considered here.

## 3. Results

In this work we considered stars with  $M = 1.0 M_\odot$  evolving from the zero-age horizontal branch (ZAHB), which corresponds to the stage after the helium flash, up to the beginning of the asymptotic giant branch. We considered self-annihilating

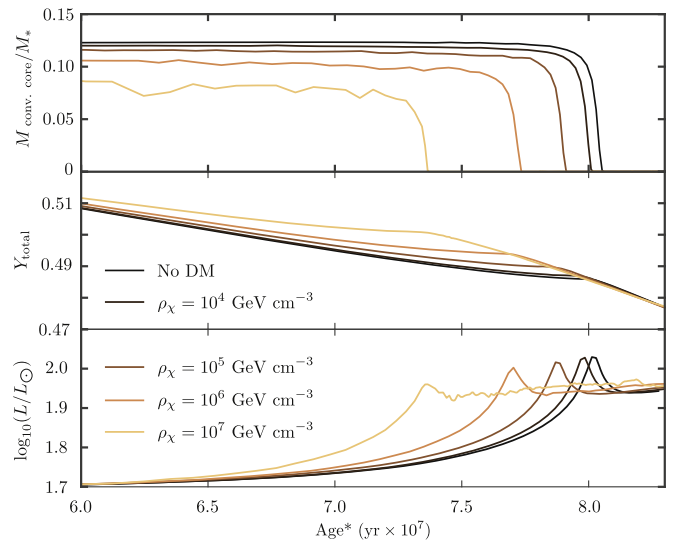


**Figure 1.** Mass of the convective core, total helium content, and total luminosity of an HB star with  $M = 1.0 M_\odot$  for different densities of DM. We considered a DM particle with  $m_\chi = 4$  GeV, spin-independent scattering cross section  $\sigma_{\chi,\text{SI}} = 10^{-39} \text{ cm}^2$  and annihilation cross section  $\langle\sigma v\rangle = 3 \times 10^{-26} \text{ cm}^3 \text{ s}^{-1}$ . The origin of the age axis corresponds to the beginning of the ZAHB (after the helium flash).

DM with the canonical thermally averaged annihilation cross section  $\langle\sigma v\rangle = 3 \times 10^{-26} \text{ cm}^3 \text{ s}^{-1}$  and a SI scattering cross section,  $\sigma_{\chi,\text{SI}} = 10^{-39} \text{ cm}^2$ . As stated before, we consider DM masses within the range  $4 \text{ GeV} < m_\chi < 10 \text{ GeV}$ . To evaluate the impact of different DM conditions on RC stars, we studied scenarios with different values of DM density. All models have solar-like metallicity and initial helium mass fraction  $Y = 0.28$ . Convection is treated according to the standard mixing length theory with  $\alpha_{\text{MLT}} = 2.0$  (Cox & Giuli 1968), and we also consider overshoot as described by Herwig et al. (1997). It should also be noted that in the conditions considered here, the capture of DM particles will always be in equilibrium with self-annihilation, i.e.,  $dN/dt = 0$ , and thus the number of DM particles in the star will be independent of the previously accumulated DM.

The effect that different DM density conditions can have on the structure and composition of an RC star are shown in Figure 1. As we can see, a star in an environment with higher DM density will have a less massive (and smaller) convective core, which is a direct consequence of the energy evacuation capacity of a large population of DM particles. As expected, the suppression of convection in the core will quench the helium in the center of the star, prompting an early end of the HB phase. This feature is evident in the total luminosity of the star, which maximum will occur earlier for models with higher  $\rho_{\text{DM}}$ , fixing a higher overall content of helium in the star at the end of the HB, as can be seen in the lower panels of Figure 1.

### 3.1. Asteroseismic Diagram

Asteroseismology studies oscillations in the stellar medium due to pressure and gravity restoration forces driven by the activity inside the star (for an introduction to asteroseismology see Aerts et al. 2010 or Basu & Chaplin 2017). In contrast to the case of solar-like stars on the main sequence, which have well-defined individual pressure and gravity modes (p- and g-modes, respectively), non-radial modes in HB stars are mixed due to the overlapping of the pressure and gravity mode

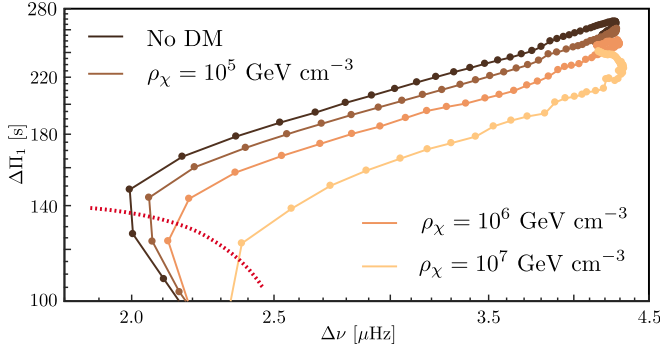


**Figure 2.** G-mode period spacing  $\Delta\Pi_1$  vs. p-mode large frequency separation  $\Delta\nu$  for an HB star with  $M = 1.0 M_\odot$  from the ZAHB phase until the beginning of the asymptotic giant branch evolved in different DM densities. The considered DM particle has  $m_\chi = 4 \text{ GeV}$ ,  $\sigma_{\chi,SI} = 10^{-39} \text{ cm}^2$  and  $\langle\sigma v\rangle = 3 \times 10^{-26} \text{ cm}^3 \text{ s}^{-1}$ . The red dashed line flags the approximate region where the HB phase ends.

cavities (Aizenman et al. 1977). Because of this coupling, mixed modes observed in HB stars allow us to extract information about the stellar structure, not only in the outer convective envelope, but also in the stellar central region. This is because they have the properties of both pressure (envelope-sensitive) and gravity (core-sensitive) modes.

Acoustic modes provide information on the outer envelope of the star and are characterized by the separation between adjacent modes with the same angular wavenumber, i.e., (Tassoul 1980)

$$\Delta\nu = \left( 2 \int_0^R \frac{dr}{c(r)} \right)^{-1}, \quad (2)$$

where  $c(r)$  is the sound speed profile and  $R$  is the radius of the star. On the other hand, g-modes, which are more sensitive to the stellar core, are characterized by their separation in period (Tassoul 1980)

$$\Delta\Pi_\ell = \frac{2\pi^2}{\sqrt{\ell(\ell+1)}} \left( \int_{r_1}^{r_2} N \frac{dr}{r} \right)^{-1}, \quad (3)$$

where  $N$  is the Brunt–Väisälä frequency, and  $\ell$  is the angular degree.

Differently from  $\Delta\nu$ , the asymptotic g-mode period spacing is computed only in between the turning points of the g-mode cavity,  $r_1$ , and  $r_2$ , which means that  $\Delta\Pi_\ell$  is directly related to the size of the convective core (Montalbán et al. 2013). The suppression of convection by DM will thus leave an imprint on the period spacing, as shown in Figure 2, where the  $\Delta\nu$ – $\Delta\Pi_1$  diagram, generally used to constrain the mass and age of giant stars (Gai et al. 2017), is shown for different values of  $\rho_{\text{DM}}$ . The g-mode period spacing will be smaller for stars within environments with increasing DM density due to the smaller size of their convective core. Moreover, if we look at  $\Delta\nu$  and  $\Delta\Pi_1$  separately as a function of the radius of the star, we can see that the large frequency separation behaves similarly between models, while the period separation is different. This behavior is expected, because g-modes are specially sensitive to the central region of the star.

### 3.2. Probing the Galactic DM Profile

The results obtained in the last section show that energy evacuation by DM can have an important effect on the g-mode

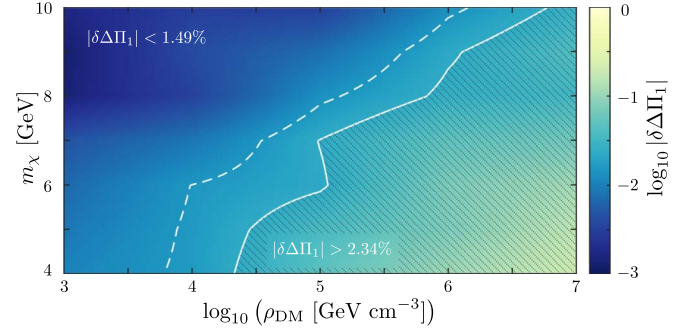


**Figure 3.** Deviation of the g-mode period separation  $\Delta\Pi_1$  in HB stars with  $M = 1.0 M_\odot$  for different  $m_\chi$  as a function of the local DM density ( $\sigma_{\chi,SI} = 10^{-39} \text{ cm}^2$  and  $\langle\sigma v\rangle = 3 \times 10^{-26} \text{ cm}^3$ ). The deviation  $\delta\Delta\Pi_1$  is computed with respect to a benchmark model obtained by fixing the input physics and removing the effects of energy transport by DM. The white contours depict the smallest (dashed) and largest (solid) relative errors in the measurement of  $\Delta\Pi_1$  in a set of 541 RC stars (Mosser et al. 2014) observed by the *Kepler* satellite. The shadowed region hence represents the region where current experiments would be sensitive to the DM impact.

period spacing of an HB star by suppressing convection in its core. As expected, the impact will be more pronounced for lower  $m_\chi$  and higher  $\rho_{\text{DM}}$ , which can be easily seen in Figure 3, where the relative deviation of the g-mode period spacing is shown as a function of the DM density for  $4 \text{ GeV} < m_\chi < 10 \text{ GeV}$ . Considering that the DM density within a galaxy can widely vary from the periphery to the galactic center, the observation of discrepancies in the g-mode period spacing of similar HB stars can be an effective way to probe the DM content of the galaxy.

To understand how the signature of DM in  $\Delta\Pi_1$  of stars in different positions of the Milky Way would compare with the precision of current asteroseismology instruments, we mapped the results shown in Figure 3 as a function of the distance to the center of the galaxy. To do this, we assume that the DM density in the Milky Way follows a generalized Navarro–Frenk–White (NFW) profile (Dahle et al. 2003),

$$\rho_{\text{gNFW}}(r) = \frac{\rho_0}{\left(\frac{r}{r_s}\right)^\gamma \left[1 + \left(\frac{r}{r_s}\right)\right]^{3-\gamma}}, \quad (4)$$

where  $r_s$  is the scale radius,  $\gamma$  is the inner slope of the profile, and  $\rho_0$  is a normalization factor. Figure 4 shows the impact of DM on the g-mode period spacing as a function of the profile’s inner slope  $\gamma$  within the range favored by recent estimations of the DM density profile in the galactic bulge (Hooper 2017).

## 4. Discussion

In the previous section, we obtained the result that RC stars embedded in large DM densities will have a smaller convective core (approximately 30% smaller in mass for  $\rho_{\text{DM}} = 10^7 \text{ GeV cm}^{-3}$  in comparison with the case where there is no energy evacuation by DM), which will ultimately result in the abrupt end of the HB phase due to a shortage in central helium. This result, which is consistent with early studies on HB stars (Dearborn et al. 1990; Salati et al. 1990), is now more relevant than ever because it will have a direct impact on the asteroseismology of the star measurable with current telescopes.

We found that HB stars in regions largely populated by DM particles will have a smaller g-mode period spacing for the

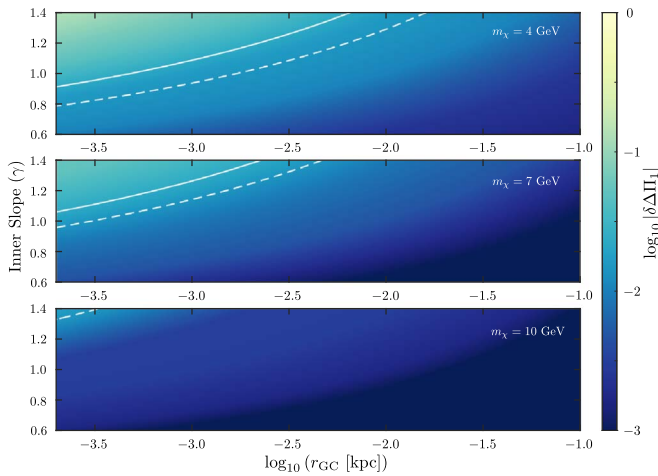


**Figure 4.** Deviation of the g-mode period separation  $\Delta\Pi_1$  in a 1 solar mass HB star as a function of the distance to the center of the galaxy. We assumed a generalized NFW profile for different values of the inner slope  $0.6 < \gamma < 1.4$ , normalized to the local DM density  $\rho_{\odot}(r_{\text{GC}} = 8 \text{ kpc}) = 0.4 \text{ GeV cm}^{-3}$  (Hooper 2017) for a DM particle with  $\sigma_{\chi,\text{SI}} = 10^{-39} \text{ cm}^2$  and  $\langle\sigma v\rangle = 3 \times 10^{-26} \text{ cm}^3 \text{ s}^{-1}$ . For the scale radius that we considered  $r_s = 10 \text{ kpc}$  (Fornasa & Green 2014).

same large frequency separation  $\Delta\nu$ . This is illustrated in Figure 3, where the relative variation of  $\Delta\Pi_1$  with respect to a benchmark model without DM is shown in a  $m_{\chi}$  versus  $\rho_{\text{DM}}$  plane. The contours represent the maximum and minimum errors in the measurement of  $\Delta\Pi_1$  of a recent experimental study comprising the analysis of 541 RC stars (Mosser et al. 2014) observed by the *Kepler* satellite, meaning that current experiments should be sensitive to the effects of DM particles within the figure’s shadowed region. Assuming a generalized NFW profile, we mapped the results to the DM distribution in the Milky Way and obtained the variation of the period spacing as a function of  $r_{\text{GC}}$ , the distance to the galactic center (see Figure 4). Rather than focusing on a specific value for the profile’s inner slope, the behavior of which is still not completely understood, we considered the range  $1.0 < \gamma < 1.5$ . As in Figure 3, contours represent an approximation to the precision of current observatories; this means that, for example, for  $m_{\chi} \simeq 4 \text{ GeV}$ , the mixed oscillation modes of RC stars in the inner parsec of the Milky Way should exhibit a measurable signature. It has also been argued that the presence of a supermassive black hole in the center of the galaxy could create a steep spike in the DM density for  $r_{\text{GC}} < 0.2 \text{ pc}$ , with  $\gamma \simeq 2.0$  corresponding to a core density of approximately  $10^9 \text{ GeV cm}^{-3}$  (Gondolo & Silk 1999), which is a few orders of magnitude above the maximum value in Figure 4.

These results illustrate how, under the assumptions considered here (i.e., a DM particle with  $m_{\chi} = 4 \text{ GeV}$ ,  $\sigma_{\chi,\text{SI}} = 10^{-39} \text{ cm}^2$ , and  $\langle\sigma v\rangle = 3 \times 10^{-26} \text{ cm}^3 \text{ s}^{-1}$ ), the asteroseismology of RC stars can be used to probe the content of DM in the Milky Way. The potential of these stars resides in the fact that their life is dictated by a convective helium-rich core highly sensitive to DM. For this reason, RC stars are more sensitive to SI interactions than main-sequence stars, including the Sun. In fact, we performed the same DM computations for a 1 solar mass star evolving from the pre-main sequence and found that in the scenarios with  $\rho_{\text{DM}} = 10^7 \text{ GeV cm}^{-3}$ , the highest DM density considered in this work, the effects of DM during the main sequence are negligible (below 0.1% in central

temperature and 0.5% in central density), and thus are not in disagreement with the standard picture of stellar evolution (i.e., without energy evacuation by DM) in stages previous to the HB.

There are, however, important sources of uncertainty inherent to our analysis. Uncertainties in the velocity distribution of DM in the halo can have an impact in the determination of the capture rate  $C_{\odot}$  (Choi et al. 2014). By considering that the velocity of the RC stars in the galactic frame is similar to the velocity of the Sun, we might be underestimating  $C_{\odot}$ , and consequently, the effects on the g-mode large period separation. Also critical is the current uncertainty in the treatment of convection transport in astrophysical contexts. As shown by Constantino et al. (2015), different mixing schemes can yield values for  $\Delta\Pi_1$  with variations up to approximately 30%. The same authors showed that the average value of the modeled g-mode large period separation is typically smaller than the observed value. Given that DM tends to decrease  $\Delta\Pi_1$  (see Figure 2), this discrepancy further increases the constraining potential of our analysis. It is important to note that, despite astrophysical uncertainties or systematic errors in the models considered here, the observation of a correspondence between the effects on  $\Delta\Pi_1$  and the distance to the galactic center (as shown in Figure 4) would provide strong support for the large concentration of DM in the central region of the Milky Way.

## 5. Conclusions

Stars in the RC have been extensively observed throughout the Milky Way and are unique astrophysical objects whose potential as a laboratory to study DM candidates has not yet been explored. In this work, we studied the effects that DM can have on the structure and evolution of these stars. We also explored the prospect of using the asteroseismology of RC stars to probe the DM content of the Milky Way. We found that energy transport by DM particles inside the star during the HB phase can help evacuate energy from the helium-burning region, leading to the suppression of convection in the outer layers of the core. This effect can have an impact on the asteroseismology of RC stars in the inner 10 pc of the Milky Way within the precision of the current experiments.

The indirect search strategy explored in this work should be considered an important complementary strategy to other direct searches (purposely built to detect DM) for multiple reasons. It allows us to test extreme environments with unique local conditions, such as the large population of DM particles near the supermassive black hole. Qualitatively, the effects studied here are relatively model independent because they are a direct consequence of a non-zero interaction cross section between DM and baryonic nuclei. Current (e.g., the *Transiting Exoplanet Survey Satellite*; Ricker et al. 2014; and the second phase of *Kepler* (K2); Stello et al. 2015) and future (e.g., the *PLANetary Transits and Oscillations of stars*; Rauer et al. 2014) asteroseismic surveys will be able to detect oscillation modes on a larger population of RC stars across the Milky Way with an unprecedented precision. Moreover, with the first imaging near-infrared (IR) surveys (*WFIRST*; Spergel et al. 2015) and the onset of asteroseismology in the IR spectrum, we will hopefully be able to observe and study RC stars in the inner parsecs of the Milky Way (which are too contaminated in the optical regime due to light from younger and more massive stars).

In the future, the identification of mixed-oscillation modes in RC stars with high precision, along with precise measurement of the star distances to the center of the galaxy, should allow us to better understand the nature and conditions of DM in the galactic center. It is also important to note that while here we considered a model of DM with a non-zero annihilation cross section, models such as asymmetric DM (where self-annihilation is negligible) should have stronger effects on the asteroseismology of RC stars, given that the population of captured DM in that scenario is usually much larger than what is considered here.

We would like to thank B. Paxton and all the team involved in the development of MESA for making the code publicly available. We would also like to thank the anonymous referee for the insightful recommendations and suggestions that contributed to improve this work. J.L. acknowledges financial support by Fundação para a Ciência e Tecnologia—FCT grant No. PD/BD/128235/2016 in the framework of the Doctoral Programme IDPASC—Portugal.

### ORCID iDs

José Lopes  <https://orcid.org/0000-0001-8249-8217>  
 Ilídio Lopes  <https://orcid.org/0000-0002-5011-9195>  
 Joseph Silk  <https://orcid.org/0000-0002-1566-8148>

### References

- Aerts, C., Christensen-Dalsgaard, J., & Kurtz, D. W. 2010, *Asteroseismology* (Dordrecht: Springer)
- Aizenman, M., Smeyers, P., & Weigert, A. 1977, *A&A*, **58**, 41
- Basu, S., & Chaplin, W. J. 2017, *Asteroseismic Data Analysis, Foundations and Techniques* (Princeton, NJ: Princeton Univ. Press)
- Casanellas, J., & Lopes, I. 2011, *ApJL*, **733**, L51
- Casanellas, J., & Lopes, I. 2013, *ApJL*, **765**, L21
- Catena, R. 2015, *JCAP*, **04**, 052
- Choi, K., Rott, C., & Itow, Y. 2014, *JCAP*, **05**, 049
- Constantino, T., Campbell, S. W., Christensen-Dalsgaard, J., Lattanzio, J. C., & Stello, D. 2015, *MNRAS*, **452**, 123
- Cox, J. P., & Giuli, R. T. 1968, *Principles of Stellar Structure* (New York: Gordon and Breach)
- Dahle, H., Hannestad, S., & Sommer-Larsen, J. 2003, *ApJL*, **588**, L73
- Dearborn, D., Raffelt, G., Salati, P., Silk, J., & Bouquet, A. 1990, *ApJ*, **354**, 568
- de Lavallaz, A., & Fairbairn, M. 2010, *PhRvD*, **81**, 123521
- Fairbairn, M., Scott, P., & Edsjö, J. 2008, *PhRvD*, **77**, 047301
- Fornasa, M., & Green, A. M. 2014, *PhRvD*, **89**, 15
- Frandsen, M. T., & Sarkar, S. 2010, *PhRvL*, **105**, 011301
- Gai, N., Tang, Y., Yu, P., & Dou, X. 2017, *ApJ*, **836**, 3
- Girardi, L. 2016, *ARA&A*, **54**, 95
- Gondolo, P., & Silk, J. 1999, *PhRvL*, **83**, 1719
- Gould, A. 1990, *ApJ*, **356**, 302
- Hekker, S., Kallinger, T., Baudin, F., et al. 2009, *A&A*, **506**, 465
- Herwig, F., Bloeker, T., Schoenberner, D., & El Eid, M. 1997, *A&A*, **324**, L81
- Hooper, D. 2017, *PDU*, **15**, 53
- Isern, J., García-Berro, E., Torres, S., & Catalán, S. 2008, *ApJL*, **682**, L109
- Jungman, G., Kamionkowski, M., & Griest, K. 1996, *PhR*, **267**, 195
- Kouvaris, C. 2008, *PhRvD*, **77**, 023006
- Lopes, I. P., Bertone, G., & Silk, J. 2002, *MNRAS*, **337**, 1179
- Lopes, J., & Lopes, I. 2016, *ApJ*, **827**, 130
- Montalbán, J., Miglio, A., Noels, A., et al. 2013, *ApJ*, **766**, 118
- Mosser, B., Benomar, O., Belkacem, K., et al. 2014, *A&A*, **572**, L5
- Paczynski, B., & Stanek, K. Z. 1998, *ApJL*, **494**, L219
- Paxton, B., Bildsten, L., Dotter, A., et al. 2011, *ApJS*, **192**, 3
- Paxton, B., Cantiello, M., Arras, P., et al. 2013, *ApJS*, **208**, 4
- Paxton, B., Marchant, P., Schwab, J., et al. 2015, *ApJS*, **220**, 15
- Paxton, B., Schwab, J., Bauer, E. B., et al. 2018, *ApJS*, **234**, 34
- Rauer, H., Catala, C., Aerts, C., et al. 2014, *ExA*, **38**, 249
- Renzini, A. 1987, *A&A*, **171**, 121
- Ricker, G. R., Winn, J. N., Vanderspek, R., et al. 2014, *Proc. SPIE*, **9143**, 914320
- Roszkowski, L., Sessolo, E. M., & Trojanowski, S. 2018, *RPPH*, **81**, 066201
- Salati, P., Raffelt, G., & Dearborn, D. 1990, *ApJ*, **357**, 566
- Salati, P., & Silk, J. 1989, *ApJ*, **338**, 24
- Scott, P., Fairbairn, M., & Edsjö, J. 2009, *MNRAS*, **394**, 82
- Spergel, D., Gehrels, N., Baltay, C., et al. 2015, arXiv:1503.03757v2
- Spergel, D. N., & Faulkner, J. 1988, *ApJL*, **331**, L21
- Spergel, D. N., & Press, W. H. 1985, *ApJ*, **294**, 663
- Steigman, G., Sarazin, C. L., Quintana, H., & Faulkner, J. 1978, *ApJ*, **83**, 1050
- Stello, D., Huber, D., Sharma, S., et al. 2015, *ApJL*, **809**, L3
- Taoso, M., Iocco, F., Meynet, G., Bertone, G., & Eggenberger, P. 2010, *PhRvD*, **82**, 121
- Tassoul, M. 1980, *ApJS*, **43**, 469
- Vincent, A. C., Scott, P., & Serenelli, A. 2015, *PhRvL*, **114**, 081302
- Zentner, A. R., & Hearin, A. P. 2011, *PhRvD*, **84**, 101302